

Supporting Information

Fluorine Substituted Organic Dyes For Efficient Dye Sensitized Solar Cells

Angela Scrascia,^a Luisa De Marco,^b Savio Laricchia,^b Rosaria Anna Picca,^c Claudia Carlucci,^{a,d} Eduardo Fabiano,^a Agostina Lina Capodilupo,^a Fabio Della Sala,^{a,b} Giuseppe Gigli,^{a,b,d} and Giuseppe Ciccarella^{a,d}*

a Istituto Nanoscienze – CNR, National Nanotechnology Laboratory (NNL), Via Arnesano, 73100 Lecce, Italy. E-mail: giuseppe.ciccarella@unisalento.it

b Center for Biomolecular Nanotechnologies @UNILE, Istituto Italiano di Tecnologia (IIT), Via Barsanti, 73010 Arnesano (LE), Italy

c Dipartimento di Scienza dei Materiali, Università del Salento, via Monteroni 73100 Lecce, Italy.

d Dipartimento di Ingegneria dell'Innovazione, Università del Salento, Via Monteroni, 73100, Lecce, Italy.

Contents

1. Absorption Spectra. Fig. S1-7 Absorption spectra of the dyes AS1-7 in different solvents and absorption spectra of dyes recorded in CHCl₃, recorded in CHCl₃ in the presence of triethylamine (TEA) and recorded in CHCl₃ in the presence of trifluoroacetic acid (TFA). Table S1. Absorption spectra data for the Dyes before and after the addition of Trifluoroacetic Acid (TFA) and Triethylamine (TEA).

Emission Spectra Fig. S8 of the dyes AS1-7.

2. Table S2. Electronic transitions.

3. Fabrication of DSSCs and photovoltaic measurements

4. NMR Spectra compounds 1a-c, 2a-c, 5-11, AS1-7

1. Absorption Spectra

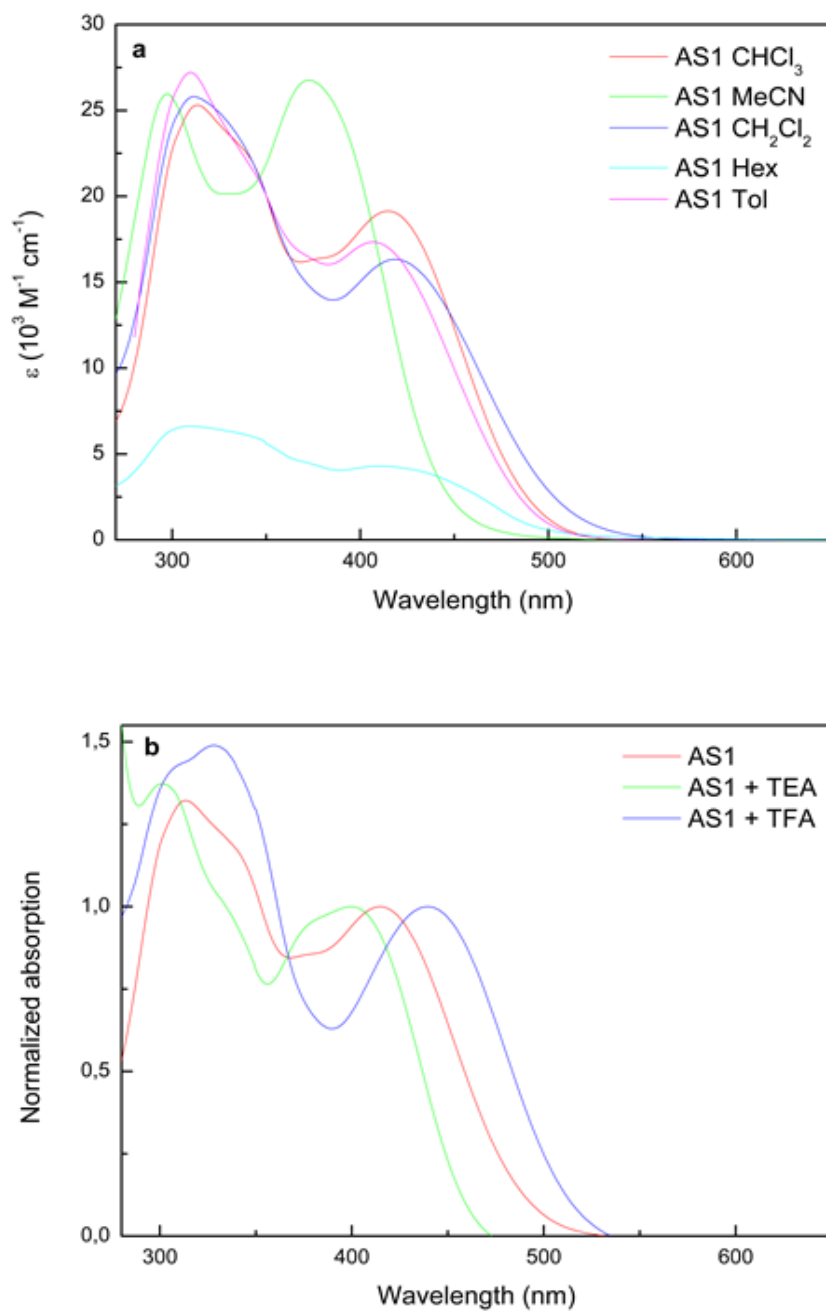


Fig. S1 Absorption spectra of the dyes **AS1** in different solvents ($3 \times 10^{-5} \text{ M}$) (a), absorption spectra of the dyes **AS1** in CHCl_3 ($3 \times 10^{-5} \text{ M}$) before (red line) and after the addition of Triethylamine (TEA) (green line) and of Trifluoroacetic Acid (TFA) (blue line) (b).

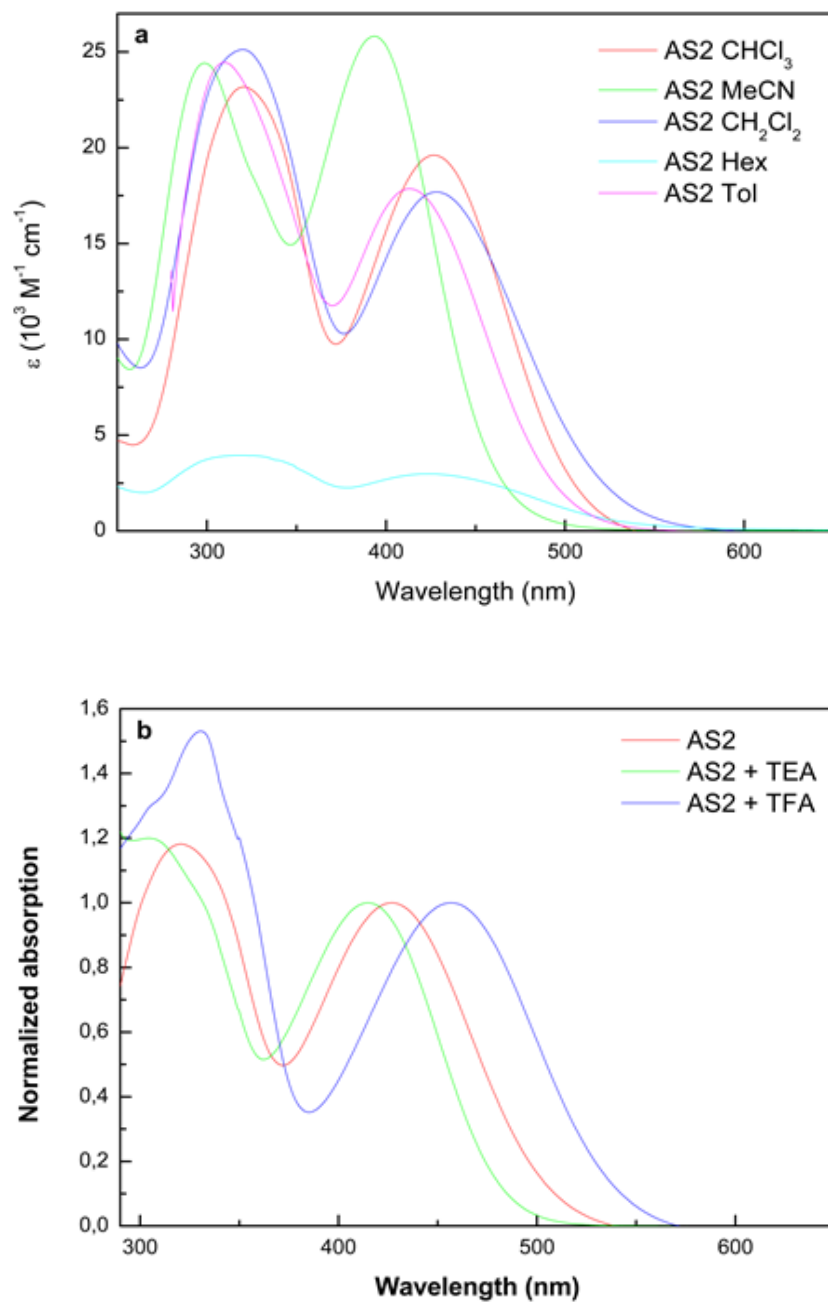


Fig. S2 Absorption spectra of the dyes **AS2** in different solvents ($3 \times 10^{-5} \text{ M}$) (a), absorption spectra of the dyes **AS2** in CHCl_3 ($3 \times 10^{-5} \text{ M}$) before (red line) and after the addition of Triethylamine (TEA) (green line) and of Trifluoroacetic Acid (TFA) (blue line) (b).

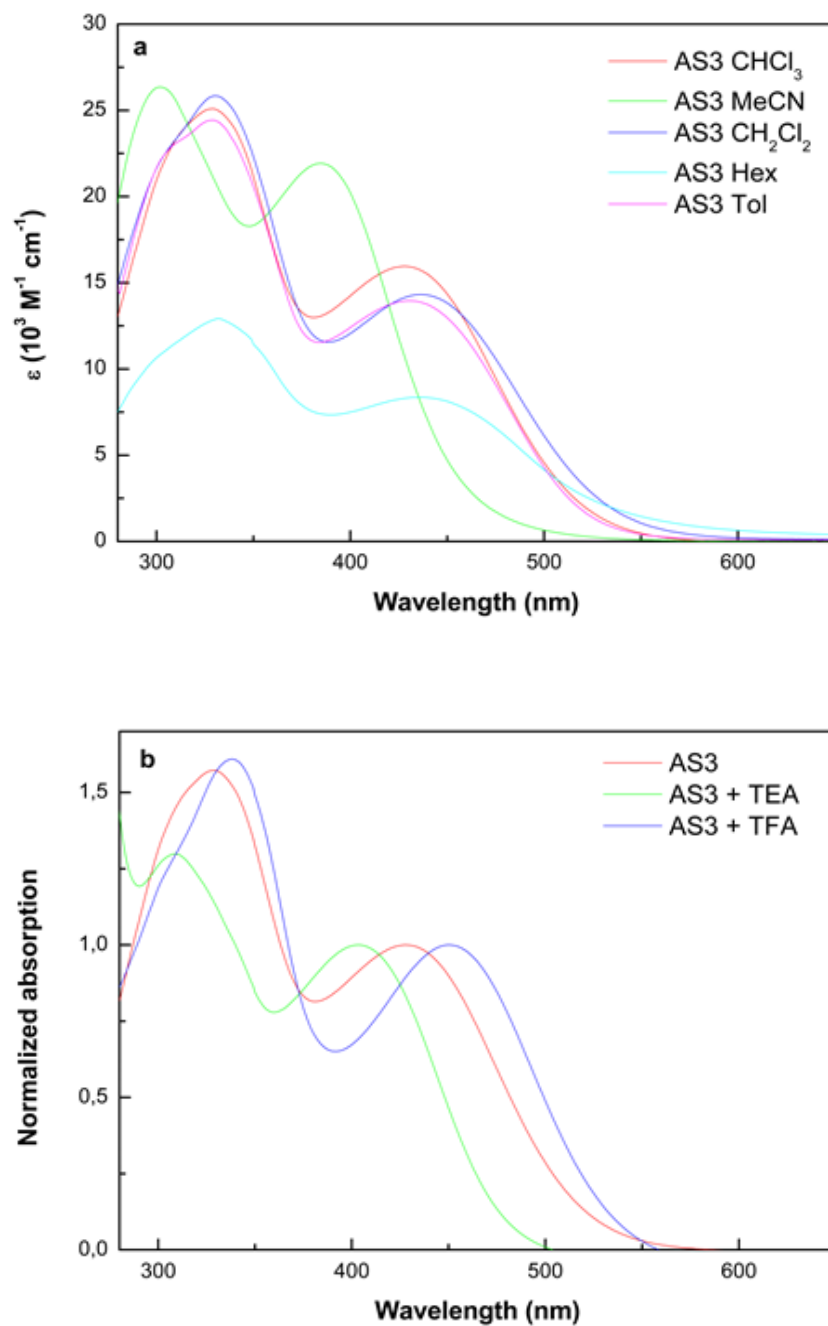


Fig. S3 Absorption spectra of the dyes **AS3** in different solvents ($3 \times 10^{-5} \text{ M}$) (a), absorption spectra of the dyes **AS3** in CHCl_3 ($3 \times 10^{-5} \text{ M}$) before (red line) and after the addition of Triethylamine (TEA) (green line) and of Trifluoroacetic Acid (TFA) (blue line) (b).

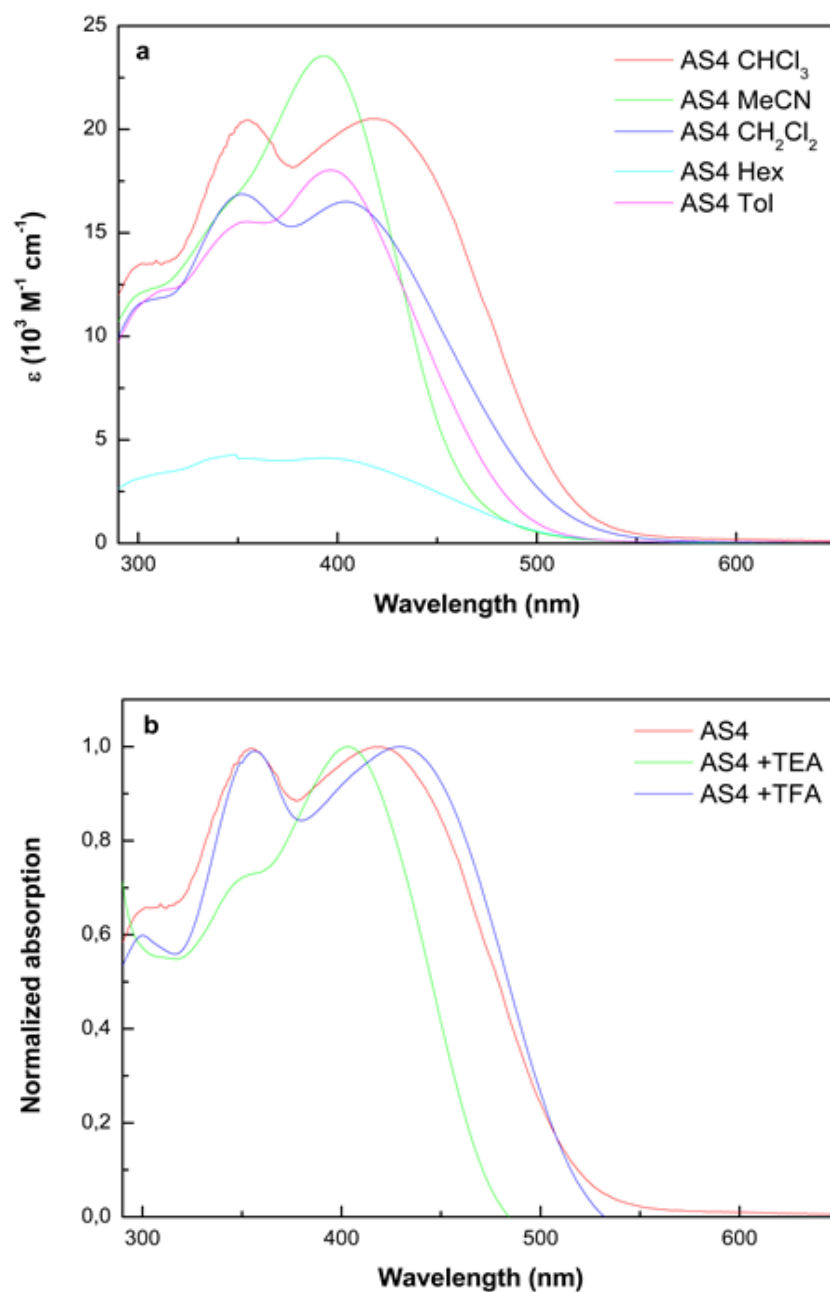


Fig. S4 Absorption spectra of the dyes **AS4** in different solvents ($3 \times 10^{-5} \text{ M}$) (a), absorption spectra of the dyes **AS4** in CHCl_3 ($3 \times 10^{-5} \text{ M}$) before (red line) and after the addition of Triethylamine (TEA) (green line) and of Trifluoroacetic Acid (TFA) (blue line) (b).

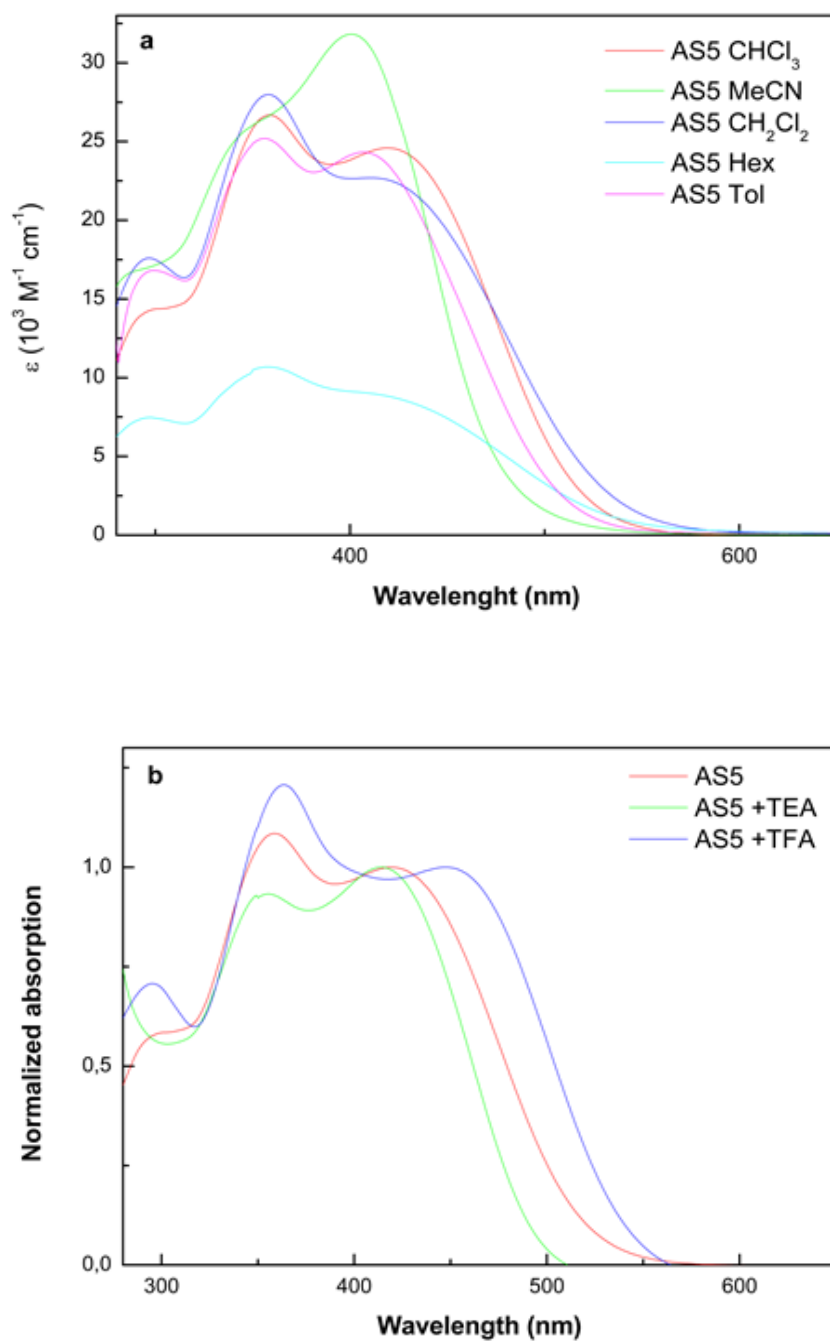


Fig. S5 Absorption spectra of the dyes **AS5** in different solvents ($3 \times 10^{-5} \text{ M}$) (a), absorption spectra of the dyes **AS5** in CHCl_3 ($3 \times 10^{-5} \text{ M}$) before (red line) and after the addition of Triethylamine (TEA) (green line) and of Trifluoroacetic Acid (TFA) (blue line) (b).

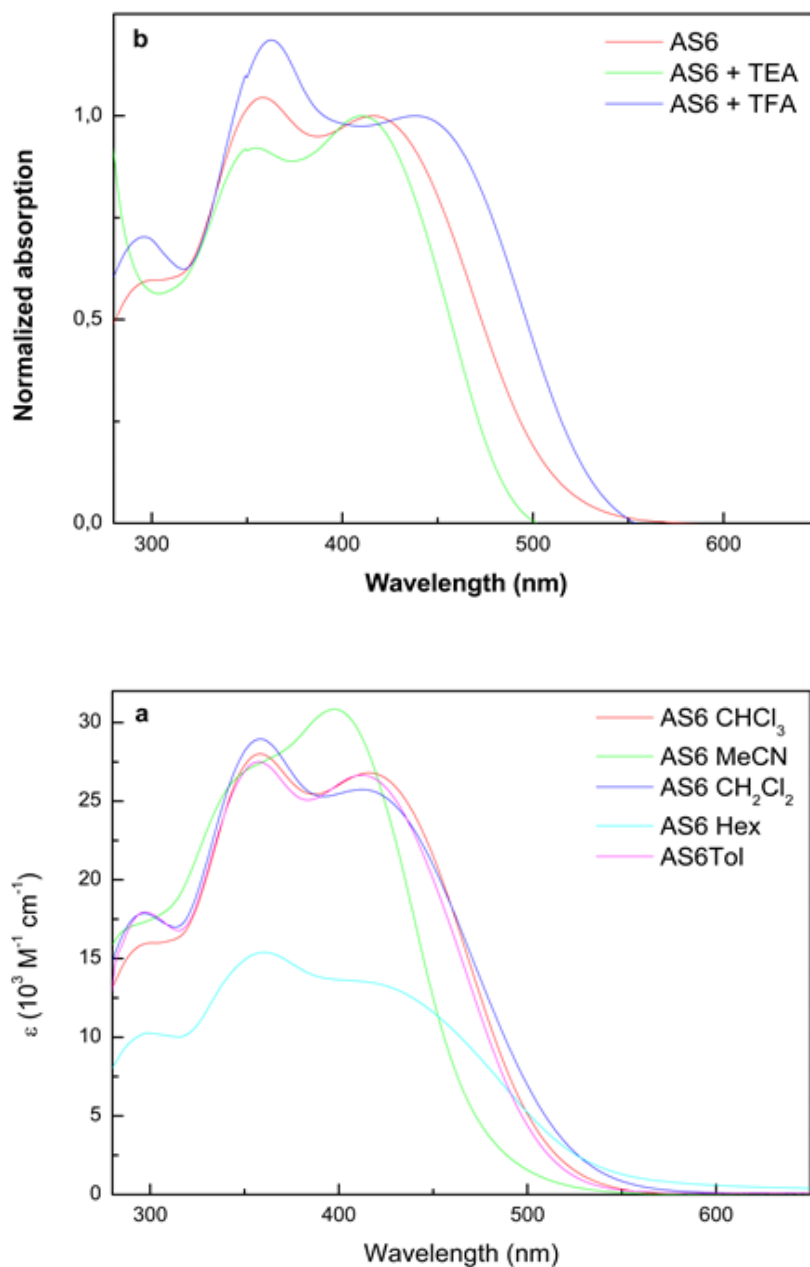


Fig. S6 Absorption spectra of the dyes **AS6** in different solvents ($3 \times 10^{-5} \text{ M}$) (a), absorption spectra of the dyes **AS6** in CHCl_3 ($3 \times 10^{-5} \text{ M}$) before (red line) and after the addition of Triethylamine (TEA) (green line) and of Trifluoroacetic Acid (TFA) (blue line) (b).

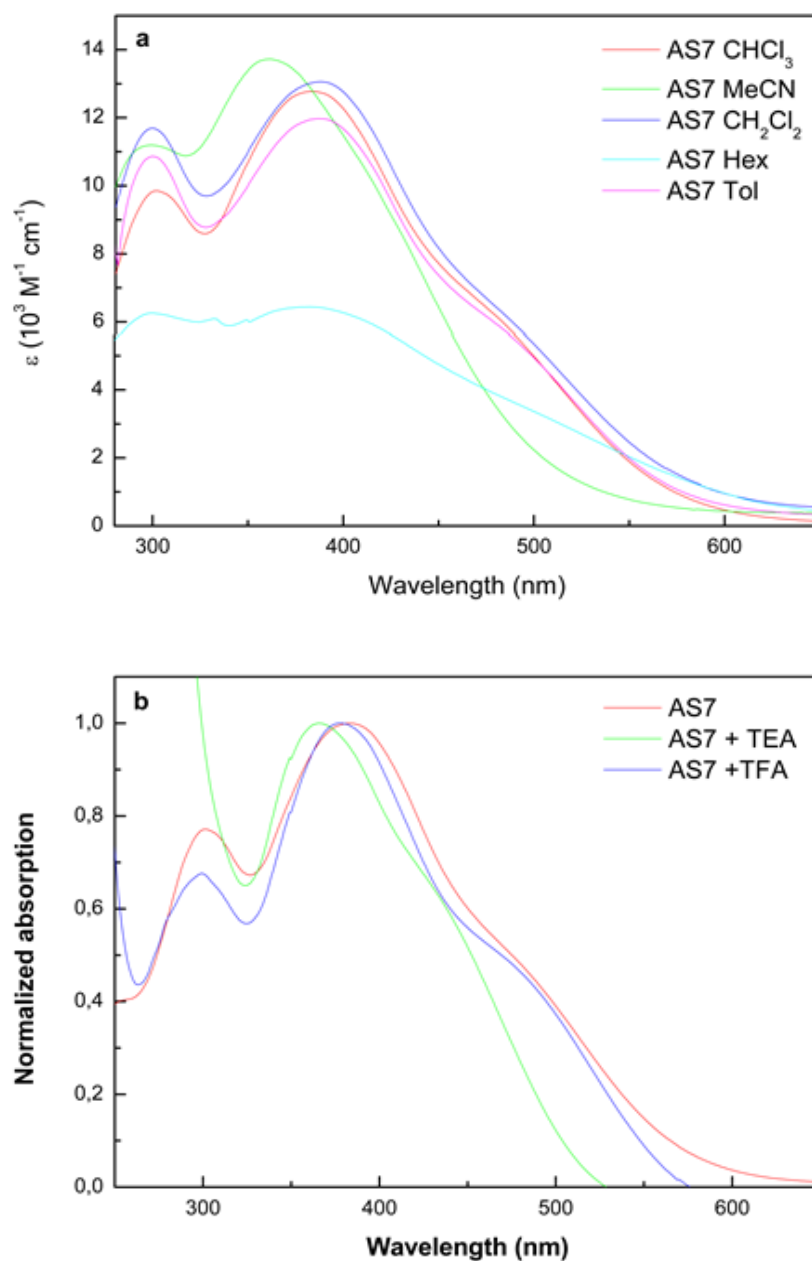


Fig. S7 Absorption spectra of the dyes **AS7** in different solvents ($3 \times 10^{-5} \text{ M}$) (a), absorption spectra of the dyes **AS7** in CHCl_3 ($3 \times 10^{-5} \text{ M}$) before (red line) and after the addition of Triethylamine (TEA) (green line) and of Trifluoroacetic Acid (TFA) (blue line) (b).

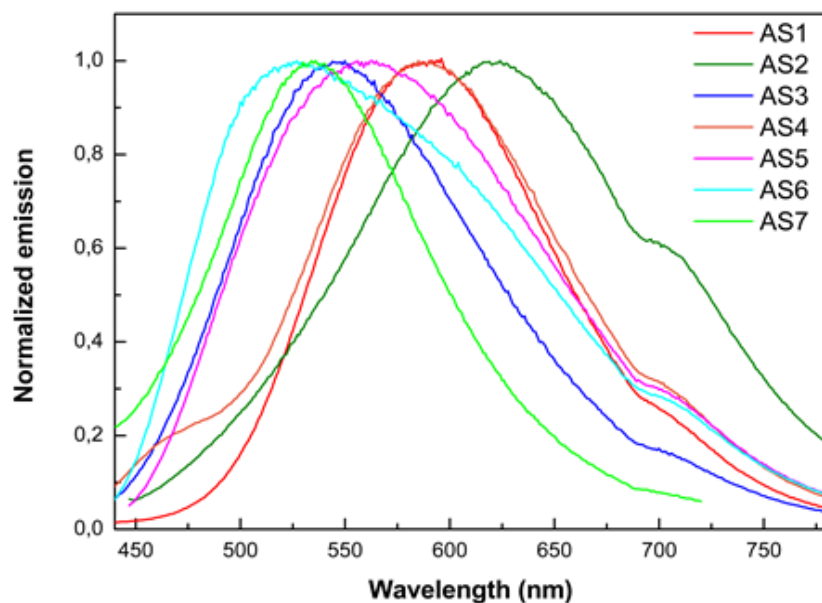


Fig. S8 Normalized Emission Spectra of the dyes **AS1-7** in different CHCl_3 .

Table S1. Absorption spectra for the Dyes before and after the addition of Trifluoroacetic Acid (TFA) and Triethylamine (TEA) and emission data.

| Dye | $\lambda_{\text{max}}/\text{nm}^{\text{a}}$ | $\epsilon/\text{M}^{-1}\text{cm}^{-1}^{\text{a}}$ | $\lambda_{\text{max}}/\text{nm}^{\text{b}}$ | $\lambda_{\text{max}}/\text{nm}^{\text{c}}$ | $\lambda_{\text{em}}/\text{nm}^{\text{a}}$ |
|------------|---|---|---|---|--|
| AS1 | 415 (313) | 19143 (25300) | 399 | 440 | 591 |
| AS2 | 427 (321) | 19614 (23180) | 415 | 457 | 624 |
| AS6 | 428 (329) | 15958 (25100) | 403 | 451 | 550 |
| AS4 | 417 (355) | 20529 (20460) | 403 | 429 | 585 |
| AS5 | 419 (358) | 24529 (26675) | 414 | 448 | 563 |
| AS6 | 416 (358) | 26798 (28009) | 410 | 438 | 527 |
| AS7 | 383 (383) | 12776 (9855) | 366 | 379 | 534 |

^aRecorded in CHCl_3 . ^bRecorded in CHCl_3 in the presence of triethylamine. ^cRecorded in CHCl_3 in the presence of trifluoroacetic acid.

2. Computational Characterization

Table S2. Calculated details of electronic transitions with the relative oscillator strengths f_{osc} obtained by performing for the **AS1** dye, in gas phase, different TD-DFT and RI-CC2 calculations.

| XC functional | Single excited state | λ (nm) | f_{osc} |
|---------------|------------------------------------|----------------|-------------------------|
| BLYP | HOMO \rightarrow LUMO (94.7%) | 712.2448 | 0.5684 |
| | HOMO -1 \rightarrow LUMO (70.5%) | 433.6638 | 1.0275 |
| | HOMO \rightarrow LUMO +1 (14.8%) | | |
| | HOMO -2 \rightarrow LUMO (48.7%) | 401.1962 | 0.1832 |
| | HOMO \rightarrow LUMO +1 (43.9%) | | |
| B3LYP | HOMO \rightarrow LUMO (99.3%) | 534.6866 | 0.8945 |
| | HOMO -1 \rightarrow LUMO (84.7%) | 369.3075 | 1.0081 |
| | HOMO \rightarrow LUMO +1 (13.8%) | | |
| | HOMO \rightarrow LUMO +2 (93.8%) | 337.7298 | 0.1182×10^{-1} |
| BHLYP | HOMO \rightarrow LUMO (81.8%) | 399.5729 | 1.6984 |
| | HOMO -1 \rightarrow LUMO (76.0%) | 299.7153 | 0.2341 |
| | HOMO \rightarrow LUMO +2 (85.1%) | 285.9950 | 0.1826×10^{-1} |
| RI-CC2 | HOMO \rightarrow LUMO (88.2%) | 425.7028 | - |
| | HOMO \rightarrow LUMO +9 (43.8%) | 320.0973 | - |
| | HOMO -1 \rightarrow LUMO (53.4%) | 310.6229 | - |

3. Fabrication of DSSCs and photovoltaic measurements

DSSC devices were prepared according to the reported literature⁶⁴⁻⁶⁶ as follows: fluorine-doped tin oxide (FTO, 10 ohm/sq., provided by Solaronix S.A.) glass plates were first cleaned in a detergent solution using an ultrasonic bath for 15 min, and then rinsed with water and ethanol. Double-layer photoanodes (thickness 13 μm) were prepared as follows: a layer of Dyesol 18NR-T paste was deposited onto FTO glass and dried at 125°C for 15 min to obtain a transparent nanocrystalline film of thickness around 8 μm ; a scattering layer, 5 μm , made by Dyesol 18-NR-AO colloidal paste was coated onto the transparent layer and the sintering process at 500°C for 30 min was performed. The active area of photoanodes was 0.16 cm^2 . The electrodes coated with the TiO_2 pastes were gradually heated under an air flow and sintered at 450 °C for 30 min. The substrate temperature was then allowed to slowly decrease. Once cooled down at about 80°C, the electrodes were immersed into 0.2 mM solutions of dyes **AS1**, **AS2**, **AS3** and **AS4** in AcCN with 3mM chenodeoxycholic acid and kept for 12 h in dark at room temperature. The reference photoanodes were prepared by dyeing into a solution 0.2 mM of (bis(tetrabutylammonium)-cis-di(thiocyanato)-N,N'-bis (4 - carboxylato - 4' - carboxylic acid-2, 2 -bipyridine) ruthenium(II) (N719, provided by Solaronix S.A.) in a mixture of acetonitrile and tert-butyl alcohol (v/v, 1:1) at room temperature for 14 h. The counter electrodes were prepared by sputtering a 50 nm Pt layer on a hole drilled cleaned FTO plate. The two plates were faced and assembled by means of a gasket of 50 μm -thick Surlyn® foil (Dyesol Ltd) interposed between them. The redox electrolyte (0.1 M LiI, 0.05 M I_2 , 0.6 M 1-methyl-3-propylimidazolium iodide, and 0.5 M tert-butylpyridine in dry acetonitrile) was vacuum-injected into the space between the electrodes. Photocurrent-voltage I-V measurements were performed using a Keithley unit (Model 2400 Source Meter). A Newport AM 1.5 Solar Simulator (Model 91160A equipped with a 300W Xenon Arc Lamp) serving as a light source. The light intensity (or radiant power) was calibrated to 100 mW/cm^2 using as reference a Si solar cell. The incident photon-to-current conversion efficiency (IPCE) was measurement by a DC method. IPCE measurements were carried out with a computerized setup consisting of a xenon arc lamp (140 W, Newport, 67005) coupled to a monochromator (Cornerstone 260 Oriel 74125). Light intensity was measured by a calibrated UV silicon photodetector (Oriel 71675) and the short circuit currents of the DSSCs were measured by using an optical power/energy meter, dual channel (Newport 2936-C).

4. NMR Spectra

